Inorg. Chem. **2003**, *42*, 5185–5191

Replacement of 2,2′-Bipyridine by 1,4-Diazabutadiene Acceptor Ligands: Why the Bathochromic Shift for $[(N\wedge N)IrCl(C_5Me_5)]^+$ Complexes but the Hypsochromic Shift for $(N\wedge N)Ir(C_5Me_5)$?

Stanislav Záliš,*,† Monika Sieger,‡ Stefan Greulich,‡ Hermann Stoll,§ and Wolfgang Kaim*,‡

J. Heyrovsky Institute of Physical Chemistry, Academy of Sciences of the Czech Republic, Dolejškova 3, CZ-18223 Prague, Czech Republic, Institut für Anorganische Chemie, Universität Stuttgart, Pfaffenwaldring 55, D-70550 Stuttgart, Germany, and Institut für Theoretische Chemie, Universität Stuttgart, Pfaffenwaldring 55, D-70550 Stuttgart, Germany

Received May 2, 2003

Replacement of 2,2′-bipyridine (bpy) by substituted 1,4-diazabutadiene (R-DAB) α-diimine ligands N∧N leads to a substantial hypsochromic shift of about 0.8 eV for the long-wavelength absorption band in compounds $(N\wedge N)Ir(C_5Me_5)$ but to a bathochromic absorption shift of about 0.4 eV for the complex ions $[(N\wedge N)IrCl(C_5Me_5)]^+$. DFT calculations on model complexes based on experimental (R-DAB compounds) and geometry-optimized structures (bpy systems) reveal that the low-energy transitions of the cationic chloro complexes are largely of ligand-to-ligand charge-transfer character L′LCT (L = α-diimine, L′ = Cl) whereas the neutral compounds exhibit $\pi \rightarrow \pi^*$ transitions between the considerably mixed metal d_π and α-diimine π^* orbitals. The much more pronounced metal–ligand orbital interaction for the R-DAB complexes causes the qualitatively different shifts on replacing the stronger basic bpy by the better π-acceptors R-DAB. Only the LUMO of the neutral compounds is destabilized on replacement of bpy by R-DAB whereas the LUMO of $[(N\wedge N)IrCl(C_5R'_5)]^+$ and both HOMOs are stabilized through this change.

Introduction

Transition metal complexes of the α-diimine chelate ligands 2,2′-bipyridine (bpy)[1] and 1,4-disubstituted 1,4-diaza-1,3-butadienes (R-DAB)[2] have been extensively studied as photosensitizers[3−6] and catalysts.[7,8]

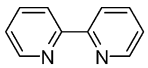

bpy

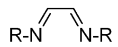

R-DAB

Whereas the electronic structures of e.g. ruthenium(II),[3] osmium(II),[4] rhenium(I),[5,7,9] platinum(II),[8,10] or copper(I)[6,11] species are well established, the rhodium and iridium catalyst systems $[(bpy)MCl(C_5Me_5)]^+/(bpy)M(C_5Me_5)$ (M = Rh or Ir) for hydride transfer[12,13] have received less attention in that respect.

Although it has long been acknowledged that the R-DAB ligands are "better" π acceptors than bpy,[2,14] the difference between corresponding classes of complexes were usually found to be quantitative rather than qualitative. During studies[15,16] of the above-mentioned components of hydride

* To whom correspondence should be addressed. E-mail: stanislav.zalis@jh-inst.cas.cz (S.Z); kaim@iac.uni-stuttgart.de (W.K.).
† Academy of Sciences of the Czech Republic.
‡ Institut für Anorganische Chemie, Universität Stuttgart.
§ Institut für Theoretische Chemie, Universität Stuttgart.

(1) McWhinnie, W. R.; Miller, J. D. *Adv. Inorg. Chem. Radiochem.* **1969**, *12*, 135.
(2) (a) Bock, H.; tom Dieck, H. *Angew. Chem.* **1966**, *78*, 549; *Angew. Chem., Int. Ed. Engl.* **1966**, *5*, 520. (b) van Koten, G.; Vrieze, K. *Adv. Organomet. Chem.* **1982**, *21*, 151 and references therein.
(3) Balzani, V.; Campagna, S.; Denti. G.; Juris, A.; Serroni, S., Venturi, M. *Coord. Chem. Rev.* **1994**, *132*, 1.
(4) (a) Kober, E. M.; Caspar, J. V.; Sullivan, B. P.; Meyer, T. J. *Inorg. Chem.* **1988**, *27*, 4587. (b) Strouse, G. F.; Schoonover, J. R.; Duesing, R.; Boyde, S.; Jones, W. E., Jr.; Meyer, T. J. *Inorg. Chem.* **1995**, *34*, 473. (c) Fetterolf, M. L.; Offen, H. W.; *J. Phs. Chem.* **1985**, *89*, 3320.
(5) Summers, D. P.; Luong, J. C.; Wrighton, M. S. *J. Am. Chem. Soc.* **1981**, *103*, 5238.
(6) (a) Cuttell, D. G.; Kuang, S.-M.; Fanwick, P. E.; McMillin, D. R.; Walton, R. A. *J. Am. Chem. Soc.* **2002**, *124*, 6. (b) Williams, R. M.; De Cola, L.; Hartl, F.; Lagref, J.-J.; Planeix, J.-M.; De Cian, A.; Hosseini, M. W. *Coord. Chem. Rev.* **2002**, *230*, 253.
(7) Hawecker, J.; Lehn, J.-M.; Ziessel, R. *Helv. Chim. Acta* **1986**, *69*, 1990.
(8) (a) Johnson, L. K.; Kilian, C. M.; Brookhart, M. *J. Am. Chem. Soc.* **1995**, *117*, 6414. (b) Johnson, L. K.; Mecking, S.; Brookhart, M. *J. Am. Chem. Soc.* **1996**, *118*, 267.
(9) Klein, A.; Vogler, C.; Kaim, W. *Organometallics* **1996**, *15*, 236.
(10) Hasenzahl, S.; Hausen, H.-D.; Kaim, W. *Chem.—Eur. J.* **1995**, *1*, 95.
(11) Vogler, C.; Kaim, W. *Z. Naturforsch.* **1992**, *47b*, 1057.

10.1021/ic034464k CCC: $25.00 © 2003 American Chemical Society
Published on Web 07/30/2003

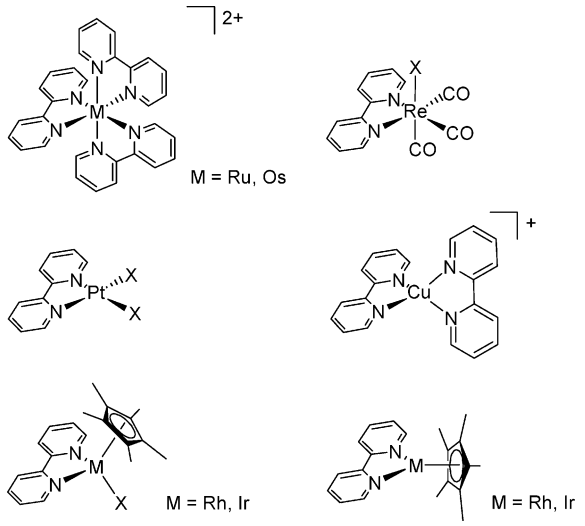

transfer catalysis cycles we have come to note a *qualitatively* very different effect on replacing bpy by R-DAB ligands in the precursor complex ions $[(N\wedge N)MCl(C_5Me_5)]^+$ and in the coordinatively unsaturated intermediates $(N\wedge N)M(C_5Me_5)$ (M = Rh, Ir):

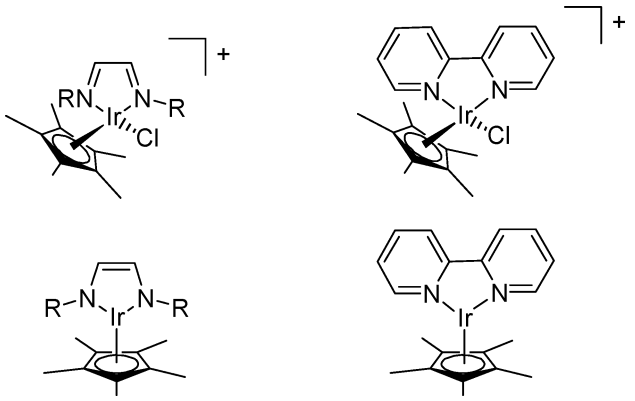

whereas a bathochromic absorption shift of about 0.4 eV could be detected for the complex ions $[(N\wedge N)IrCl(C_5Me_5)]^+$, a substantial hypsochromic shift of ca. 0.8 eV was observed for the long-wavelength absorption band in compounds $(N\wedge N)Ir(C_5Me_5)$. Scheme 1 summarizes this for representative examples,[16,17] and Figure 1 shows spectra of R-DAB complexes.

To understand these puzzling observations we have now undertaken DFT calculations for the iridium systems for which some structural data are available.[17] While the cationic complexes $[(N\wedge N)IrCl(C_5Me_5)]^+$ are clearly identified as iridium(III) species, the situation is less obvious for neutral $(N\wedge N)Ir(C_5Me_5)$: on the basis of structural information for the case with R = 2,6-dimethylphenyl (Xyl), the (R-DAB) compounds were interpreted as enediamido−iridium(III) complexes $(R\text{-}DAB^{-II})Ir^{III}(C_5Me_5)$[17] while the corresponding bpy complex was tentatively formulated with *effective* oxidation states of +II for the metal and −I for the bpy ligand.[16] This interpretation was based on the appearance of weak long-wavelength near-infrared bands with the typical vibrational splitting observed for $bpy^{\bullet-}$ and its complexes.[18] The extraordinary *negative* shifts of the reduction potentials on coordination of bpy or R-DAB with $M(C_5Me_5)$ were seen as supporting this interpretation, suggesting very strong metal/ligand orbital π back-donation.[15−17] Although all four kinds of complexes exhibit absorptions in the visible region (Scheme 1), the nature of the low-energy transitions remained unclear. We therefore attempted not only to resolve the origin of the dichotomous bpy/R-DAB effect but also to establish the assignment of these transitions.

Computational Details

Ground-state electronic structure calculations have been done by density-functional theory (DFT) methods using the ADF2000.2[19,20] and Gaussian 98[21] program packages. The lowest excited states of the closed-shell complexes were calculated by the time-dependent DFT (TD-DFT) method (both ADF and G98 programs).

Within the ADF program, Slater type orbital (STO) basis sets of triple-ζ quality with polarization functions were employed. The inner shells were represented by the frozen core approximation (1s for C, N, 1s−2p for Cl, and 1s−4d for Ir were kept frozen). The

(12) (a) Kölle, U.; Grätzel, M. *Angew. Chem.* **1987**, *99*, 572; *Angew. Chem., Int. Ed. Engl.* **1987**, *26*, 568. (b) Kölle, U.; Kang, B.-S.; Infelta, P.; Compte, P.; Grätzel, M. *Chem. Ber.* **1989**, *112*, 1869. (c) Cosnier, S.; Deronzier, A.; Vlachopoulos, N. *J. Chem. Soc., Chem. Commun.* **1989**, 1259. (d) Rodriguez, M.; Romero, I.; Llobet, A., Deronzier, A.; Biner, M.; Parella, T.; Stoeckli-Evans, H. *Inorg. Chem.* **2001**, *40*, 4150. (e) Laguitton-Pasquier, H.; Martre, A.; Deronzier, A. *J. Phys. Chem. B* **2001**, *105*, 4801. (f) Chardon-Noblat, S.; Deronzier, A.; Ziessel, R. *Collect. Czech. Chem. Commun.* **2001**, *66*, 207. (g) Chardon-Noblat, S.; Deronzier, A.; Hartl, F.; Van Slageren, J.; Mahabiersing, T. *Eur. J. Inorg. Chem.* **2001**, 613. (h) Chardon-Noblat, S.; Cripps, G. H.; Deronzier, A.; Field, J. S.; Gouws, S.; Haines, R.; Southway, F. *Organometallics* **2001**, *20*, 1668. (i) Romero, I.; Collomb, M.-N.; Deronzier, A.; Llobet, A.; Perret, E.; Pecaut, J.; Le Pape, L.; Latour, J.-M. *Eur. J. Inorg. Chem.* **2001**, 69.
(13) (a) Ziessel, R. *J. Am. Chem. Soc.* **1993**, *115*, 118. (b) Ziessel, R. *Angew. Chem.* **1991**, *103*, 863; *Angew. Chem., Int. Ed. Engl.* **1991**, *30*, 844.
(14) tom Dieck, H.; Franz, K.-D.; Hohmann, F. *Chem. Ber.* **1975**, *108*, 163.
(15) Ladwig, M.; W. Kaim, W. *J. Organomet. Chem.* **1991**, *419*, 233.
(16) (a) Ladwig, M.; Kaim, W. *J. Organomet. Chem.* **1992**, *439*, 79. (b) Kaim, W.; Reinhardt, R.; Sieger, M. *Inorg. Chem.* **1994**, *33*, 4453. (c) Kaim, W.; Reinhardt, R.; Waldhör, E.; Fiedler, J. *J. Organomet. Chem.* **1996**, *524*, 195. (d) Bruns, W.; Kaim, W.; Ladwig, M.; Olbrich-Deussner, B.; Roth, T.; Schwederski, B. In *Molecular Electrochemistry of Inorganic, Bioinorganic and Organometallic Compounds*; Nato ASI Series C 385; Pombeiro, A. J. L., McCleverty, J., Eds.; Kluwer Academic Publishers: Dordrecht, The Netherlands, 1993; p 255.
(17) (a) Greulich, S., Kaim, W.; Stange, A. F.; Stoll, H.; Fiedler, J.; Záliš, S. *Inorg. Chem.* **1996**, *35*, 3998. (b) Greulich, S.; Klein, A.; Knoedler, A.; Kaim, W. *Organometallics* **2002**, *21*, 765.
(18) (a) Shida, T. *Electronic Absorption Spectra of Radical Ions*; Elsevier: Amsterdam, 1988; p 197. (b) Braterman, P. S.; Song, J.-I.; Kohlmann, S.; Vogler, C.; Kaim, W. *J. Organomet. Chem.* **1991**, *411*, 207. (c) Braterman, P. S.; Song, J.-I.; Wimmer, F. M.; Wimmer, S.; Kaim, W.; Klein, A.; Peacock, R. D. *Inorg. Chem.* **1992**, *31*, 5084.
(19) Fonseca Guerra, C.; Snijders, J. G.; Te Velde, G.; Baerends, E. J. *Theor. Chim. Acc.* **1998**, *99*, 391.
(20) van Gisbergen, S. J. A.; Snijders, J. G.; Baerends, E. J. *Comput. Phys. Commun.* **1999**, *118*, 119.
(21) Frisch, M. J.; Trucks, G. W.; Schlegel, H. B.; Scuseria, G. E.; Robb, M. A.; Cheeseman, J. R.; Zakrzewski, V. G.; Montgomery, J. A., Jr.; Stratmann, R. E.; Burant, J. C.; Dapprich, S.; Millam, J. M.; Daniels, A. D.; Kudin, K. N.; Strain, M. C.; Farkas, O.; Tomasi, J.; Barone, V.; Cossi, M.; Cammi, R.; Mennucci, B.; Pomelli, C.; Adamo, C.; Clifford, S.; Ochterski, J.; Petersson, G. A.; Ayala, P. Y.; Cui, Q.; Morokuma, K.; Malick, D. K.; Rabuck, A. D.; Raghavachari, K.; Foresman, J. B.; Cioslowski, J.; Ortiz, J. V.; Stefanov, B. B.; Liu, G.; Liashenko, A.; Piskorz, P.; Komaromi, I.; Gomperts, R.; Martin, R. L.; Fox, D. J.; Keith, T.; Al-Laham, M. A.; Peng, C. Y.; Nanayakkara, A.; Gonzalez, C.; Challacombe, M.; Gill, P. M. W.; Johnson, B. G.; Chen, W.; Wong, M. W.; Andres, J. L.; Head-Gordon, M.; Replogle, E. S.; Pople, J. A. *Gaussian 98*, revision A.7; Gaussian, Inc.: Pittsburgh, PA, 1998.

Scheme 1

$[(R\text{-}DAB)IrCl(C_5Me_5)]^+$	$[(bpy)IrCl(C_5Me_5)]^+$
green	yellow
λ_{max} = 580 nm (ε = 350 M^{-1} cm^{-1})	440 nm (sh)
425 nm (3200)	349 nm
-2e⁻, + Cl⁻ E_{pa} = -0.35 V vs $Fc^{+/o}$ ⇅ + 2e⁻, - Cl⁻ E_{pc} = -0.80 V	-2e⁻, + Cl⁻ E_{pa} = -1.04 V ⇅ + 2e⁻, - Cl⁻ E_{pc} = -1.55 V
(R-DAB)Ir(C_5Me_5)	(bpy)Ir(C_5Me_5)
orange	purple
431 nm (10000)	737 nm
	672 nm
R = Xyl = 2,6-dimethylphenyl	617 nm
	530 nm (sh)
	494 nm

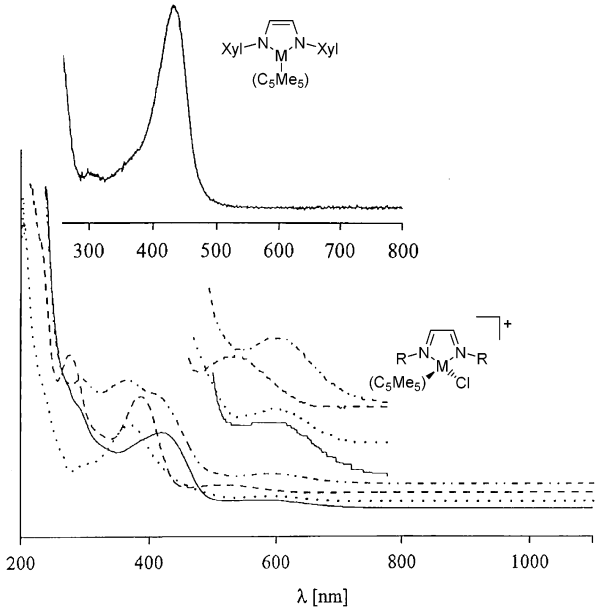

Figure 1. Absorption spectra of organoiridium complexes with R-DAB ligands.[17] Lower scale: Spectra of $[(R\text{-}DAB)IrCl(C_5Me_5)](PF_6)$ in CH_3CN (R = Xyl (−), cyclohexyl (---), *p*-tolyl (···), *o*-tolyl (·•---)). Upper scale: Spectrum of (Xyl-DAB)Ir(C_5Me_5) in toluene. (Absorbance values are different for each spectrum.)

following density functionals were used within ADF: the local density approximation (LDA) with VWN parametrization of electron gas data or the functional including Becke's gradient correction[22] to the local exchange expression in conjunction with Perdew's gradient correction[23] to LDA correlation (ADF/BP). Compositions and energies of molecular orbitals as well as electronic transition energies and their composition were calculated by the asymptotically correct SAOP functional[24] (ADF/SAOP) which is more accurate for higher-lying MOs and electronic transitions. Core electrons were included in the ADF/SAOP calculations. The scalar relativistic (SR) zero-order regular approximation (ZORA) was used within this study.

Within Gaussian-98 Dunning's polarized valence double-ζ basis sets[25] were used for C, N, Cl, and H atoms and the quasirelativistic effective core pseudopotentials and corresponding optimized set of basis functions[26] for Ir. Becke's hybrid three-parameter functional together with the Lee, Yang, and Parr correlation functional (B3LYP)[27] was used in Gaussian 98 calculations (G98/B3LYP).

Throughout the calculations the C_5Me_5 ligand was replaced by C_5H_5. Calculations on R-DAB complexes were done with R = CH_3. The calculations were performed within C_s-constrained symmetry (*xz* as the symmetry plane).

Results and Discussion

The cationic complexes $[(N\wedge N)IrCl(C_5Me_5)]^+$ and neutral $(N\wedge N)Ir(C_5Me_5)$ are connected by a chloride-dissociative two-electron reduction (EEC or ECE process) which is chemically reversible.[12−16] The main experimental absorption maxima[16,17] for the bpy and R-DAB systems are given in Scheme 1; other experimental absorption data are summarized further below together with the calculation results (Table 5). For simplification, the cyclopentadienide coligand was used in unsubstituted form in the calculations and the substituent R = Me in R-DAB.

Geometry Optimization. Geometry optimization of the Me-DAB/C_5H_5-containing model systems using ADF/BP reproduces the essential experimental characteristics of the

(22) Becke, A. D. *Phys. Rev. A* **1988**, *38*, 3098. Becke, A. D. *Phys. Rev. A* **1988**, *38*, 3098.
(23) Perdew, J. P. *Phys. Rev. A* **1986**, *33*, 8822.
(24) Schipper, P. R. T.; Gritsenko, O. V.; van Gisbergen, S. J. A.; Baerends, E. J. *J. Chem. Phys.* **2000**, *112*, 1344.
(25) Woon, D. E.; Dunning, T. H. J. *J. Chem. Phys.* **1993**, *98*, 1358.
(26) Andrae, D.; Haeussermann, U.; Dolg, M.; Stoll, H.; Preuss, H. *Theor. Chim. Acta* **1990**, *77*, 123.
(27) Stephens, P. J.; Devlin, F. J.; Cabalowski, C. F.; Frisch, M. J. *J. Phys. Chem.* **1994**, *98*, 11623.

Table 1. Experimental and ADF/BP-Calculated Selected Bond Lengths (Å) and Angles (deg) of R-DAB Complexes

	[(R-DAB)Ir($C_5R'_5$)]		[(R-DAB)IrCl($C_5R'_5$)]$^+$	
	calcd[a]	expt[b]	calcd[a]	expt[b]
Ir−N	1.983	1.977	2.066	2.091
Ir−Cl			2.377	2.354
Ir−C	2.237−2.247	2.174−2.204	2.224−2.243	2.215−2.198
$(N-C)_{DAB}$	1.366	1.373	1.297	1.288
$(C-C)_{DAB}$	1.377	1.334	1.449	1.445
N−Ir−N	77.0	76.9	76.6	76.0
Ir−N−C	118.0	116.8	115.5	115.3
$(N-C-C)_{DAB}$	113.5	113.6	115.6	115.3
N−Ir−Cl			86.0	86.9

[a] Calculated for R = Me and R′ = H. [b] Experimental values for R = Xyl and R′ = Me.[17]

Table 2. ADF/BP Calculated Selected Bond Lengths (Å) of bpy Complexes

	[(bpy)Ir(C_5H_5)]	[(bpy)IrCl(C_5H_5)]$^+$
Ir−N	1.967	2.048
Ir−Cl		2.377
Ir−C_{cp}	2.256−2.278	2.226−2.233
N−C2	1.395	1.365
N−C6	1.375	1.352
C2−C2′	1.428	1.469

Xyl-DAB/C_5Me_5 compounds. Bond lengths and angles calculated by using G98/B3LYP do not differ substantially from those obtained with ADF/BP. An improvement relative to the previous ab initio approach with H-DAB model complexes[17] can be noted especially for the charged chloride-containing precursor complex. In fact, the longer calculated C−C distance within the R-DAB ligand of (N∧N)Ir($C_5R'_5$) indicates a lesser degree of metal-to-ligand electron transfer in the Me-DAB model, probably due to the lower π-acceptor capability of alkyl-DAB in relation to aryl-DAB ligands. Nevertheless, the values still support the iridium(III) oxidation state description according to (R-DAB^{-II})Ir^{III}($C_5R'_5$) (Table 1). Similar enediamido(2−) ligand structures were observed for several main group species[28] and for some early transition metal complexes.[29] On the other hand, the geometry optimization for (bpy)Ir(C_5H_5) reveals a less pronounced metal-to-ligand electron transfer. Especially the most indicative inter-ring bond distance of bpy[30] is calculated at 1.428 Å and thus not that *much* shorter than the single bond of 1.469 Å calculated for [(bpy)IrCl(C_5H_5)]$^+$ (Table 2). The 1.428 Å value for C2−C2′ is certainly longer than what may be expected for a C═C double bond at the center of dianionic bpy^{2-}.[30]

Molecular Orbital Energies and Compositions. The eventually calculated transition energies are based on the MO energies from optimized geometries. The MO schemes of the four model complexes and the frontier orbitals of the Me-DAB compounds are illustrated in Figures 2−5; a detailed characterization in terms of symmetry, energy, and composition is given for the most relevant MOs in Tables 3 and 4.

If one starts with the cationic systems [(N∧N)IrCl(C_5H_5)]$^+$, the calculations yield a π*(N∧N)-based LUMO for both the

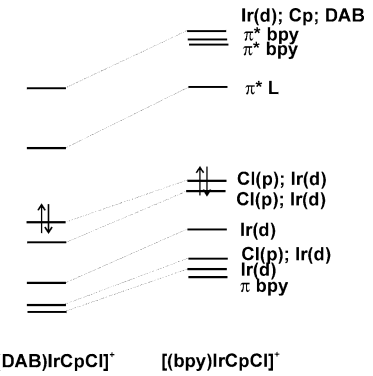

Figure 2. MO schemes for model complex cations [(N∧N)IrCl(C_5H_5)]$^+$ from DFT calculations (DAB = Me-DAB).

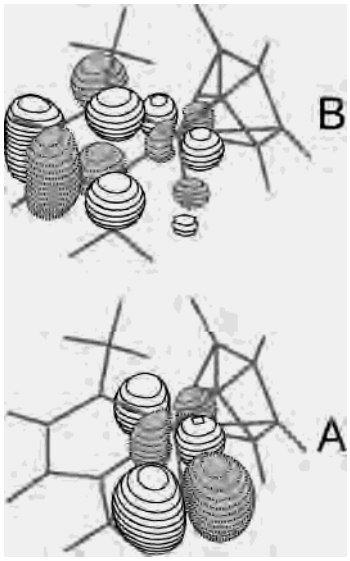

Figure 3. Representations of the frontier orbitals of [(Me-DAB)IrCl(C_5H_5)]$^+$ from DFT calculations: A, HOMO (55a′); B, LUMO (56a′).

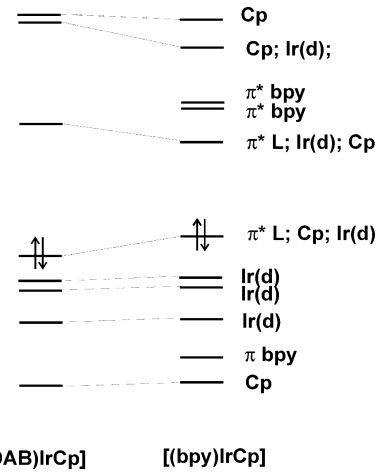

Figure 4. MO schemes for model complexes [(N∧N)Ir(C_5H_5)] from DFT calculations (DAB = Me-DAB).

(28) Schmidt, E. S.; Jockisch, A.; Schmidbaur, H. *J. Am. Chem. Soc.* **1999**, *121*, 9758 and literature cited.

(29) (a) Mashima, K.; Matsuo, Y.; Tani, K. *Organometallics* **1999**, *18*, 1471. (b) Matsuo, Y.; Mahsima, K.; Tani, K. *Angew. Chem.* **2001**, *113*, 986; *Angew. Chem., Int. Ed.* **2001**, *40*, 960.

(30) (a) Chisholm, M. H.; Huffman, J. C.; Rothwell, I. P.; Bradley, P. G.; Kress, N.; Woodruff, W. H. *J. Am. Chem. Soc.* **1981**, *103*, 4945. (b) Fedushkin, I. L.; Petrovskaya, T. V.; Girgsdies, F.; Köhn, R. D.; Bochkarev, M. N.; Schumann, H. *Angew. Chem.* **1999**, *111*, 2407; *Angew. Chem., Int. Ed.* **1999**, *38*, 2262.

bpy and Me-DAB species (Table 3, Figures 2 and 3). Due to the lower π^* level and higher LUMO coefficients at the N-coordination centers for DAB ligands,[14] the stabilization on going from bpy- to R-DAB-containing cationic complexes is quite pronounced (Figure 2).

The HOMO is composed mainly of p(Cl) and d(Ir) orbitals (Figure 3) which is also stabilized albeit to a lesser extent on going from the bpy to the R-DAB complex. The calculation with the hybrid B3LYP functional indicates slightly larger d(Ir) contributions to the a′ HOMO for both complexes. The origin of this comparatively small effect is the weaker σ donor capability of R-DAB in comparison to bpy.[14] Taken together, the HOMO−LUMO difference is smaller for the R-DAB system, in agreement with the lower energy of this σ(Ir−Cl) → π^*(N∧N) transition in the experiment for the cations $[(N\wedge N)IrCl(C_5Me_5)]^+$ (cf. Table 5).

In contrast to the cationic systems where HOMO and LUMO are not extensively mixed, the neutral species $(N\wedge N)Ir(C_5H_5)$ are calculated with a very different electronic situation (Table 4, Figures 4 and 5): the frontier orbitals result from an extensive, symmetry-supported interaction between the α-diimine π^* MO and the corresponding electron-rich d_π orbital (d_{xz}) of the initial d^8 fragment $Ir(C_5H_5)$. The distinctly stronger interaction in the Me-DAB complex with its much smaller α-diimine π system inevitably results in a considerably larger HOMO−LUMO gap than for the bpy analogue and, by extension, to a corresponding HOMO → LUMO transition at much higher energy (cf. Table 5). This DFT-based interpretation explains the very substantial difference between the $(R\text{-DAB})Ir(C_5Me_5)$ and $(bpy)Ir(C_5Me_5)$ compounds (Scheme 1) and is also in agreement with the redox potential differences $E_{pa}(ox) - E_{pc}(red)$ from processes (1) and (2) which are 1.83 V for N∧N = bpy[16] but 2.87 V for N∧N = Xyl-DAB.[17]

$$[(N\wedge N)Ir(C_5Me_5)] - 2e^- \xrightarrow{E_{pa}(ox)} [(N\wedge N)Ir(C_5Me_5)]^{2+} \quad (1)$$

$$[(N\wedge N)Ir(C_5Me_5)] + e^- \overset{E_{pc}(red)}{\rightleftharpoons} [(N\wedge N)Ir(C_5Me_5)]^- \quad (2)$$

If one views all four MO schemes (Figures 2 and 4), it is remarkable that only the LUMO of the neutral compounds is destabilized on replacement of bpy by R-DAB whereas the LUMO of $[(N\wedge N)IrCl(C_5H_5)]^+$ and both HOMOs are stabilized through this change.

Electronic Transitions. Results from TD-DFT calculations using both the ADF/SAOP or the G98/B3LYP approach are summarized together with experimental data in Table 5.

Beginning with the cationic chloride complexes $[(N\wedge N)IrCl(C_5Me_5)]^+$, we had previously[16,17] speculated whether the lowest transitions observed were due to either Cl^--to-N∧N or $C_5Me_5^-$-to-N∧N charge transfer. The surprising low-energy shift of the typically green R-DAB complexes in comparison to the yellow-orange bpy analogues was a main reason for undertaking this study.

As the TD-DFT calculation results from Table 5 in conjunction with Tables 3 and 4 suggest, the long-wavelength bands in the visible of the cationic complexes are mainly caused by chloride-to-α-diimine transitions with some metal involvement (Ir−Cl bond) and the π^*(N∧N) LUMO as target orbital. This kind of transition has similarly been found in organometallic complexes of the α-diimine ligands where it was at times referred to as ligand-to-ligand charge transfer (L′LCT)[10] or σ bond-to-ligand charge transfer (SBLCT).[31] In agreement with the experiment these bands are calculated with a relatively low intensity, probably reflecting poor orbital overlap. The second major transition is due to a metal-to-ligand charge transfer (MLCT), followed by another L′LCT (bpy complex). Whereas the agreement of absolute energy values from ADF/SAOP is excellent for the R-DAB example, each of the two observed bands of the bpy complex seems to involve two transitions which did not allow us to exactly ascertain the accuracy of the two methods used.

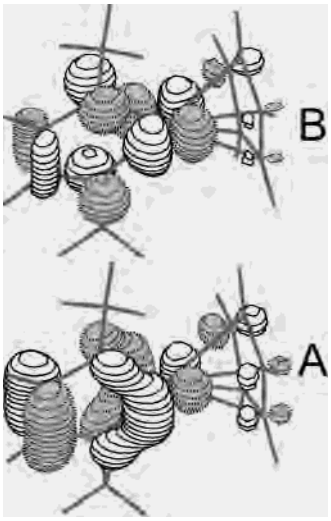

Figure 5. Representations of the frontier orbitals of $[(Me\text{-}DAB)Ir(C_5H_5)]$ from DFT calculations: A, HOMO (49a′); B, LUMO (50a′).

For a proper description of the low-energy transitions of the neutral species $(N\wedge N)Ir(C_5Me_5)$, we must further differentiate. As an intriguing result of the calculations, we are now able to obtain a more quantitative extent of the different degrees of metal−ligand π orbital mixing in relation to the aforementioned associated geometrical effects in these complexes. The R-DAB systems appear to exhibit a rather complete transfer of two electrons from the metal to the π-acceptor ligand, confirming the experimental structure and oxidation state description for $(R\text{-}DAB^{-II})Ir^{III}(C_5Me_5)$, R = 2,6-dimethylphenyl (Table 1). Accordingly, the TD-DFT method confirms the occurrence of one intense transition at rather high energy (Table 5). The transition energy of the model is calculated at slightly higher value than the experimentally observed absorption; however, in agreement with previous arguments the character of the transition is π → π^* (HOMO → LUMO) with a somewhat higher ligand character of the HOMO and rather high metal contribution

(31) van Slageren, J.; Klein, A.; Zalis, S. *Coord. Chem. Rev.* **2002**, *230*, 193.

Table 3. ADF/SAOP-Calculated One-Electron Energies and Percentage Composition of Selected Highest Occupied and Lowest Unoccupied MOs of $[(N\wedge N)IrCl(C_5H_5)]^+$, Expressed in Terms of Composing Fragments[a]

MO	*E* (eV)	prevailing character	Ir	Cl	Cp	bpy/Me-DAB
			N∧N = bpy			
unoccupied						
67a′	−9.57	Ir(d); bpy; Cp	28 (d)	11	18	52
42a″	−9.65	bpy	9 (d)		8	72
66a′	−9.74	bpy; Cp	13 (d)	9	10	67
65a′	−10.52	bpy π^*	4 (d)	2		92 (π^*)
occupied						
41a″	−12.48	Cl(p) + Ir(d)	34 (d)	53	7	4
64a′	−12.72	Cl(p) + Ir(d)	28 (d)	62		6
63a′	−13.34	Ir(d)	36 (d)	28	20	9
40a″	−13.90	Cl(p) + Ir(d)	24	30	4	42
62a′	−14.20	Ir(d)	2 (s); 65 (d)	14	4	7
39a″	−14.07	bpy	9	11	3	76
			N∧N = Me-DAB			
unoccupied						
33a″	−9.77	Ir(d), Cp; Cl	28 (d)	18	33	8
57a′	−10.29	Ir(d), Cp; DAB	45 (d)		30	23
56a′	−11.52	π^* DAB	15 (d)	7 (p)		76 (π^*)
occupied						
32a″	−13.19	Cl(p) + Ir(d)	29 (d)	63	2	6
55a′	−13.52	Cl(p) + Ir(d)	15 (d)	72		8
54a′	−14.07	Ir(d)	46 (d)	15	20	15
31a″	−14.62	Cl(p) + Ir(d)	31	41	8	9
53a′	−14.81	Ir(d)	2 (s); 1 (p); 51 (d)	14	8	6

[a] Cp = C_5H_5.

Table 4. ADF/SAOP-Calculated One-Electron Energies and Percentage Composition of Selected Highest Occupied and Lowest Unoccupied MOs of $[(N\wedge N)Ir(C_5H_5)]$, Expressed in Terms of Composing Fragments[a]

MO	*E* (eV)	prevailing character	Ir	Cp	bpy/Me-DAB
		N∧N = bpy			
unoccupied					
41a″	−4.09	Ir; Cp; bpy	48 (d)	24	27
60a′	−5.26	π^* bpy; Ir(d)	14 (d)	6	79
40a″	−5.32	π^* bpy	2 (d)	3	95
59a′	−5.87	π^* bpy; Ir(d); Cp	15 (d)	10	75 (π^*)
Occupied					
58a′	−7.37	π^* bpy; Ir(d); Cp	3 (p); 23 (d)	22	51
57a′	−8.48	Ir(d)	9 (s); 78 (d)	7	5
39a″	−8.54	Ir(d)	76 (d)	7	16
56a′	−9.20	Ir(d)	5 (s); 87 (d)	3	4
38a″	−9.66	bpy	2 (d)		97
37a″	−9.92	Cp	1 (p); 5 (d)	72	21
		N∧N = Me-DAB			
unoccupied					
51a′	−3.33	Ir(d); Cp; DAB	30 (d)	55	23
31a″	-3.99	Cp; DAB	3 (d)	73	23
50a′	−5.60	π^* DAB; Ir(d); Cp	36 (d)	20	43 (π^*)
occupied					
49a′	−7.78	π^* DAB; Ir(d); Cp	17 (d)	22	61
30a″	−8.50	Ir(d)	67 (d)	9	23
48a′	−8.67	Ir(d)	9 (s); 74 (d)	10	6
47a′	−9.25	Ir(d)	6 (s); 82 (d)	4	6
29a″	−9.99	Cp	7 (d)	73	19

[a] Cp = C_5H_5.

to the LUMO, approaching an LMCT situation as would be appropriate for a formulation $(R\text{-}DAB^{-II})Ir^{III}(C_5R'_5)$.

On the other hand, the geometry optimization for $(bpy)Ir(C_5H_5)$ with a moderately diminished inter-ring distance of bpy has already pointed to a less extensive $d_\pi(Ir)-\pi^*(N\wedge N)$ orbital interaction with only partial metal-to-ligand electron transfer in the ground state. Much in agreement with the ADF/SAOP calculated values there are now three main transitions in the visible, each of $\pi \rightarrow \pi^*$ character with some MLCT contribution. Whereas there are three different π^*(bpy) target orbitals involved, all three of these transitions start from the HOMO of mixed metal/ligand composition. The original hypothesis[16,17] of an effective one-electron charge transfer in the ground state from the metal to the bpy ligand in $(bpy)Ir(C_5Me_5)$ appears to be confirmed. Thus, there is not only a DFT-reproduced enormous low-energy shift of the long-wavelength transitions on changing from R-DAB to bpy in complexes $(N\wedge N)Ir(C_5R_5)$; there is also a crucial change in character of that $\pi \rightarrow \pi^*$ transition from a more LMCT-like situation for the R-DAB systems to a more MLCT-resembling condition in the bpy case. Strong metal/ligand orbital mixing occurs for the (destabilized) LUMO

Table 5. Selected Calculated Lowest TD-DFT Singlet Transition Energies and Oscillator Strengths for Complexes

		ADF/SAOP		G98/B3LYP		
state	main composn (%) and CT character	trans energy[a]	osc str[b]	trans energy[a]	osc str[b]	Expt E_{max} (λ_{max})/ϵ[c]
		[(bpy)IrCl($C_5R'_5$)]$^+$				
$^1A'$	94 (64a′ → 65a′); L′LCT	2.34 (529)	0.018	3.04 (408)	0.015	2.82 (440)
$^1A'$	58 (63a′ → 65a′); 26 (64a′ → 66a′); MLCT	2.97 (417)	0.023	3.41 (368)	0.009	
$^1A'$	68 (64a′ → 66a′); 19 (63a′ → 65a′); L′LCT	3.05 (406)	0.016	3.29 (377)	0.014	3.55 (349)
$^1A'_1$	90 (41a″ → 42a″); L′LCT	3.38 (367)	0.024	3.63 (342)	0.030	
		[(Me-DAB)IrCl($C_5R'_5$)]$^+$				
$^1A'$	85 (55a′ → 56a′); 14 (54a′ → 56a′); L′LCT	2.21 (561)	0.005	2.58 (481)	0.008	2.14 (580)/350
$^1A'$	76 (54a′ → 56a′); 12 (53a′ → 56a′); MLCT	2.94 (422)	0.033	3.24 (383)	0.054	2.92 (425)/3210
$^1A_1$	94 (55a′ → 57a′); 4 (53a′ → 56a′)	3.39 (365)	0.054	3.87 (320)	0.062	
$^1A'$	66 (53a′ → 56a′); 20 (32a″ → 33a″)	3.45 (359)	0.011	3.45 (359)	0.018	
		[(bpy)Ir($C_5R'_5$)]				
$^1A'$	73 (58a′ → 59a′); 26 (58a′ → 60a′); $\pi \rightarrow \pi^*$/MLCT	1.91 (649)	0.031	2.09 (594)	0.071	1.68 (740) sh,[d] 1.85 (670),[d] 2.01 (618)[d]
$^1A''$	90 (58a′ → 40a″); 5 (39a″ → 59a′); $\pi \rightarrow \pi^*$/MLCT	2.41 (514)	0.059	2.67 (464)	0.068	2.33 (533)
$^1A'$	61 (58a′ → 60a′); 19 (58a′ → 59a′); 13 (39a″ → 40a″); $\pi \rightarrow \pi^*$/MLCT	2.68 (462)	0.133	2.82 (440)	0.172	2.53 (490)
$^1A''$	86 (39a″ → 59a′); 11 (58a′ → 40a″)	2.84 (436)	0.027	2.85 (434)	0.018	
$^1A'$	83 (39a″ → 40a″); 8 (58a′ → 60a′)	3.57 (347)	0.229	4.21 (294)	0.131	
		[(Me-DAB)Ir($C_5R'_5$)]				
$^1A'$	93 (49a′ → 50a′); 2 (48a′ → 50a′); $\pi \rightarrow \pi^*$/LMCT	3.22 (388)	0.209	3.25 (381)	0.205	2.88 (431)/10 000
$^1A''$	97 (30a″ → 50a′)	3.25 (382)	0.012	3.03 (409)	0.009	
$^1A'$	97 (47a′ → 50a′)	3.82 (328)	0.001	3.72 (337)	0.018	

[a] Transition energies in eV (corresponding wavelengths in nm), calculated for R = Me and R′ = H. [b] Only transitions with oscillator strengths >0.001 are listed. [c] Absorption maxima in eV (or nm), molar extinction coefficients ϵ in M^{-1} cm^{-1} (from refs 16,17); R = Xyl, R′ = Me. [d] Vibrationally structured band (ref 16).

of the R-DAB complex and for the HOMOs of both compounds. Such metal/ligand orbital mixing appears to facilitate efficient two-electron catalysis due to the created charge buffer capacity. However, the individual electronic situation must be considered in each case as demonstrated here by the surprising difference between the bpy and R-DAB complex analogues.

Acknowledgment. This work was supported through the COST D14 program of the European Union, through the Deutsche Forschungsgemeinschaft (DFG), the Fonds der Chemischen Industrie, and the Ministry of Education of the Czech Republic (Grant OC.D 14.20).

IC034464K